Structural Health Monitoring For Unmanned Aerial Systems

Yong Keong Yap

Electrical Engineering and Computer Sciences
University of California at Berkeley

Technical Report No. UCB/EECS-2014-70
http://www.eecs.berkeley.edu/Pubs/TechRpts/2014/EECS-2014-70.html

May 14, 2014

Acknowledgement

The author would like to thank Professor Raja Sengupta from UC Berkeley for stimulating discussion and guidance throughout the course of this Master's Project. Also, special thanks go to 3D Robotics for loaning the equipment required for flying and testing the drones. The author would also like to thank Professor Kris Pister's group at UC Berkeley for agreeing to loan out their IMUs and Atmel RZUSBSticks. Finally, heartfelt thanks go to Fabien Chriam, a graduate student with Pister's group, for his guidance and advice on speeding up and optimizing the data collection process with the IMUs, Python and MATLAB scripts.

University of California, Berkeley College of Engineering

MASTER OF ENGINEERING - SPRING 2014

Electrical Engineering and Computer Science

Physical Electronics & Integrated Circuits

STRUCTURAL HEALTH MONITORING FOR UNMANNED AERIAL SYSTEMS

YONG KEONG YAP

This **Masters Project Paper** fulfills the Master of Engineering degree requirement.

Approved by:

1. Capstone Project Advisor:

Signature: _____ Date _____

Print Name/Department: RAJA SENGUPTA/CIVIL AND ENVIRONMENTAL ENGINEERING

2. Faculty Committee Member #2:

Signature: _____ Date _____

Print Name/Department: PIETER ABBEEL/ELECTRICAL ENGINEERING AND COMPUTER SCIENCES

ABSTRACT

Currently, drones are not very reliable systems. This paper presents a sensor system to detect motor defects on drones to overcome this deficiency. The feasibility of installing micro-electromechanical (MEMS) accelerometers on drones to inspect the vibration characteristics of a drone is investigated. Accelerometers were installed near the drone motors to collect vibration data and a Fourier Fast Transform (FFT) was used to analyze the data. An empirical method of observing the vibration spectrum of an Unmanned Aerial Systems (UAS) airframe was demonstrated by adopting motor vibration measurement methods. A baseline condition for what constitutes proper operation was first made. Airframes that were intentionally damaged showed significant differences in vibration spectrum, demonstrating that a cheap and feasible failure prediction and detection warning system can be applied to small scale UAS.

I: INTRODUCTION

Unmanned Aerial Systems (UAS) are flying robots that require little or no human control while flying. Also known as drones, these flying machines have gained infamy for their effectiveness in military strike roles [1,2]. In particular, UAS has shown to be effective at conducting missions that are “dull and dirty”, since they can be programmed to do boring tasks for an extended amount of time, especially in fields such as surveillance and patrolling [1, 2].

The effectiveness of UAS in the military space has drawn the attention of companies beyond the military realm. There has been a rise in companies that want to use UAS for purposes such as freight, video taking or surveillance. In particular, farmers have been scrutinizing the ability of UAS to replace manned aircraft for the purposes of surveying large acreage of crops at a lower price point and more convenience [3, 4]. In more recent cases, there have been

companies interested in using this technology for the purposes of delivering cargo to customers. For example, Amazon.com Inc. in 2013 revealed that it is investigating the feasibility of using UAS to deliver small packages to customers fast [5], as well as Lakemaid, an beer brewery in Alaska, testing out an aerial beer delivery system [6]. In a report, the Association for Unmanned Vehicles and Systems International projected the global civilian UAS market to grow from $4.2B USD in 2015 to $82B USD in 2025 [7, 8].

Despite the promise of the technology, UAS on sale on the civilian market are not very reliable currently. They lack collision sensing mechanisms, self diagnosis of structural integrity, and are flown by a group of hobbyists who may or may not have proper training on the safety issues from these machines. A hair-raising incident of a near-collision between a UAS and a civilian airliner in 2013 brought these safety concerns to the forefront [9]. As a consequence, the Federal Aviation Authority (FAA), which regulates and oversees US airspace, imposed a blanket ban on commercial UAS applications other than hobbyists flying it below 400 feet and weighting less than 55 pounds [10, 11]. Therefore, despite the interest in UAS, adoption has not taken off.

The work presented in this paper aims to demonstrate a low cost warning system on UAS to overcome this lack of reliability. Specifically, the work targets the monitoring of motors using their vibration data. By attaching accelerometers in close proximity to the motors being monitored, we can get a sense of the motors' state of health in preflight tests as well as potentially in real time as the machines are flying. As a result, we may be able to then trigger a warning whenever the readings from the motors seem to indicate an impending failure. This would alleviate concerns about reliability of UAS as an industry.

Currently, there has been ongoing work on UAS in many different aspects. The most popular ones are the automation of landing and takeoff, as well as navigation using computer

vision and GPS. Ceres Imaging, a California based startup working on UAS imaging, is trying to provide spectral data from UAS flying over farms to optimize water and fertilizer use on crops [12]. Another startup, Skycatch, is targeting agriculture and mining applications by providing an entire system which features a truly autonomous UAS. Skycatch is working to provide a UAS capable of conducting surveillance missions intelligently [13].

In the field of structural reliability monitoring, not much has been done on UAS specifically. Currently on the hobbyists' platform, there is a battery and radio link monitoring system. If the battery is low or the radio link to the ground station is lost, some versions of UAS can be set to automatically goes into a fail-safe mode and returns to its origin [14]. Previous work has been done on monitoring the health of motors by inspecting a variety of their mechanical and electrical behavior [15, 16, 17]. In [15], motor bearings were shown to cause vibration and noise due to varying stiffness and the distribution of defects in the bearings. This is due to the bearings acting as discrete rolling bodies that roll around along the raceways of a given motor. The number of rolling bearings and the speed of the rolling give rise to radial vibrations, which usually occur as a harmonic multiple of the motor speed. Also, Sunnersjö [16] explained in detail how variations in bearing size due to defects give rise to axial vibration, and how these vibrations are seen in the vibration spectrum as harmonics of bearing rotation. He further explained how the increased contact forces from the vibrations cause more wear and tear, hastening the failure process. In [17], signal processing techniques were applied to the vibration spectrum of helicopter gearboxes to separate the vibrations due to the gears and the bearings. In particular, Randall [17] pointed out the difficulties of measuring the vibration spectrum when it is strongly masked by vibration from the gears, which typically cover "the whole of the audio frequency range". Furthermore, Randall added that due to modulation between different

vibration mechanisms, the spectrum can get very convoluted, requiring special demodulation and filtering techniques to process the data. This problem can be circumvented, however. Ma and Li [18] demonstrated the use of demodulation of vibration data to deduce the defects on gears. In their experiments, the high frequencies of gear rotations were mixed with the relatively lower frequencies of defects passing through a contact region. They modeled the number of gears and how the vibration spectrum would change as a function of the number and type of defects on the gears. This idea can potentially be applied to cases with different vibration sources generating different frequencies on an UAS.

Apart from measuring the vibration data directly, one can also measure the electrical current flow through a motor to deduce its state of health. Schoen et. al. [19] made use of electromagnetic induction on the stator coils within the brushless motors to determine their rotational speed, thus deducing how much vibration is generated. By modeling the rotation of the bearings and the contact forces between the bearings and the raceways, the authors managed to characterize different defects 4-pole induction motors with different loading conditions. Riley et. al. [20] furthered the idea by measuring a baseline current measurement and vibration measurement for a motor operating normally. The authors then verified a linear relationship between the vibration and current readings. They then used the current readings primarily to extrapolate the vibration data while the motor was in use, eliminating the need for an external sensor.

Tandon and Choudhury [21] summarize the vibration analysis methods in use in modern day to diagnose or detect failures in rolling bearings. Despite the extensive amount of past work they mentioned, little work has been done for the specific application of UAS motor monitoring. In [15, 16, 19], work was done only on large scale industrial motors. These motors can easily

incorporate accelerometers and acoustic sensors in their structure due to their size, either by manufacturing the sensors into the motor, or just by attaching the sensors onto the motors when in use. Unfortunately, in the case of UAS motors, we are investigating small scale motors with diameters of at most 3 inches across. This scale makes it difficult, if not impossible, to mount accelerometers in the manner as in [15, 16]. At the same time, the nature of vertical flight in quadcopters also implies vertical accelerations in the plane of a motor. More precisely, the vibrations along the shaft of a motor are not just due to the bearings and rotations. The vibrations can also arise due to coupling from their immediate environment, such as propeller loading and balancing, vibration due to other motors on the same airframe as well as an 8-10 Hz oscillation due to the presence of a flight stabilization loop controlling the aircraft. All the above points mentioned imply that in order to capture vibration data during flight, it may be more insightful to capture vibrations arising from not only the motors, but the structure of the airframe as well.

The work in this paper aims to apply the techniques from mechanical vibration analysis of motors on small platforms such as UAS. In particular, we adopt the idea from [19] of measuring and then using a baseline condition to compare against real time measurements. However, instead of measuring the stator current like in [19], we chose to measure and analyze the vibration of a normal motor. Also, instead of measuring the vibration *on the motor*, we chose to measure the vibration *on the airframe,* near the motor. This is because of the small size of the motor, as well as the hope that we can capture structural failure apart from those of the motor. For example, if the vertical axis vibrations get significantly larger on one quadcopter arm, one can infer that the screws holding down the arm are coming loose, rather than the motor failing.

By analyzing the vibration spectrum, we hope to diagnose mechanical problems when they are not serious. In general, increased vibrations from a small defect will cause increased

wear on load bearing parts and rotating bearings, worsening the problem and accelerating the failure. By providing a technique to show problems as they arise or even before something serious happens, we hope to improve the safety of using UAS in any civilian airspace.

Section II of the paper deals with the methods and materials we used, as well as the methodology behind our motor health monitoring tool. The set up will be created to simulate environments similar to an actual flying UAS. Section III contains results of the experiments, including plots of the time domain and FFT data of the motor vibrations. Section IV contains discussion about the results and the implications. The implication will cover the implications on a company looking to provide UAS platforms for customers, from a technological and cost point of view. Section V includes our conclusions. Section VI and section VII are the acknowledgements and list of literature cited respectively.

II: METHODS AND MATERIALS

In order to characterize the motor vibrations and diagnose potential failure, a set up to measure vibration data from a motor was needed. The sensor should be able to measure acceleration data, weigh as little as possible, and not interfere with the airflow around a motor/propeller combination. A motor functioning properly should be characterized first. Motors with defective structures are then characterized and compared against the ideal case.

For the purpose of an experiment, an inertial measurement unit (IMU) was attached to the drone shaft, near the motor. It is tightly bound to the shaft by non-conductive tape. The IMU is a 2.5cm x 3cm printed circuit board featuring an accelerometer, magnetometer, gyroscope, temperature sensor, microcontroller, as well as 2.4 GHz radio transceiver. It is a board developed at Kris Pister's lab at the University of California, Berkeley [22]. While the IMU is overdesigned

for more general uses, for the work in this paper, only the accelerometer was used to collect vibration data.

The accelerometer used is a LIS344ALHTR MEMS accelerometer manufactured by STMicroelectronics. It measures acceleration data within a ±2g range and gives an analog voltage output between 0V to 3.3V. The Texas Instruments MSP430F2618 microcontroller then took in the readings through its 12 bit analog-digital converter (ADC). The MSP430 functions at 16 MHz and samples the ADC at 1 KHz. The readings were then transmitted by the Atmel AT86RF231 radio. An Atmel RZUSBstick 2.4 GHz transceiver plugged into a PC running Windows 8 received the acceleration data and sent it to the PC through the serial port running at a baudrate of 921600.

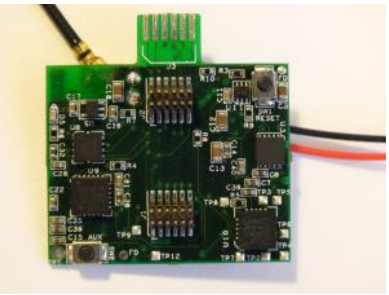

Figure 1. Inertial Measurement Unit Used (Source: OpenWSN GINA Project [22])

For the purpose of visualizing the vibration of the motors under different conditions, a series of sub experiments were done. First, an Atmel Atmega 328P microcontroller was used to generate a 50 Hz Pulse Width Modulation (PWM) signal. This signal was then sent to the Electronic Speed Controller (ESC). The ESC was loaded with SimonK firmware and is sold by 3DRobotics. The ESC then converted the PWM signal and sent it to an 850 KV, 14 pole, 12 stator, brushless motor, also sold by 3DRobotics. The ESC is powered by a high discharge rate 3-cell lithium polymer battery at a nominal voltage of 11.1V. A series of static tests were

conducted using this setup on the ground, both with a load and without a load. For the loaded case, the motor was loaded by a 10x4.7 propeller.

Data points were the motor was spinning at its low speed setting (4% and 4.5% duty cycle, 800us and 900us pulse width), moderate speed setting (9% and 9.5% duty cycle, 1800us and 1900us pulse width), as well as at its high speed (11% and 11.5% duty cycle, 2200us and 2300us pulse width). Next, the motor was artificially given some common "failure modes". For example, the screws holding down the pylon to the motor were loosened slightly to allow for wobbling of the propeller. A set of readings were collected using this set up. Next, the motor was slightly loosened after tightening the pylons back, and another set of readings were obtained. Finally, a broken propeller was attached onto the motor for the same speed tests.

Figure 2. Broken Propeller.

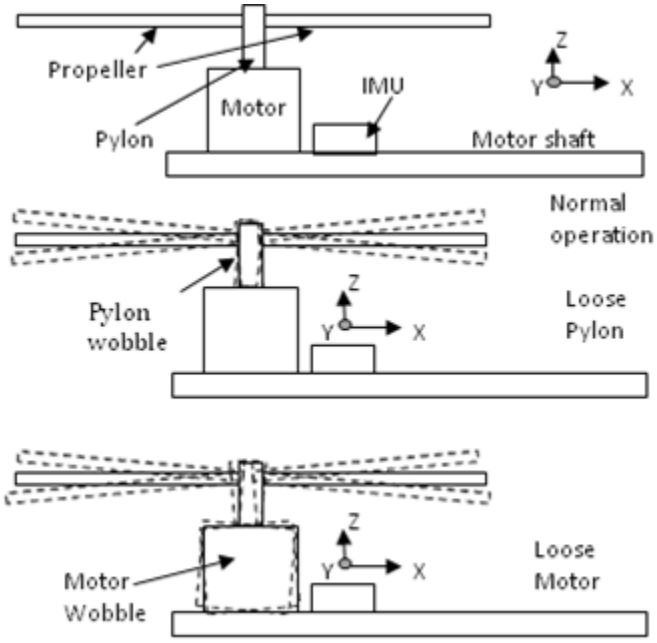

Figure 3. Set ups for static tests.

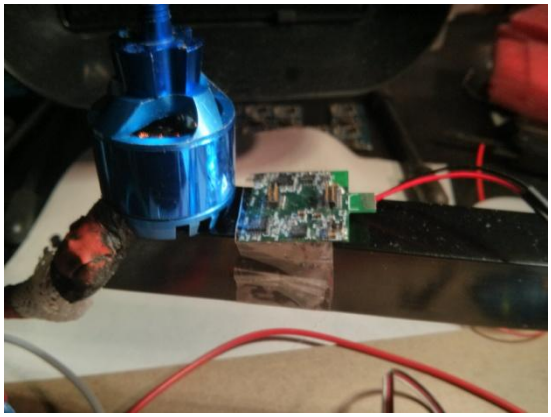

Figure 4. IMU on motor shaft.

After the above setups, an actual flight test was done. The IMU was mounted at the same position on a quadcopter drone. The drone was powered by the Ardupilot open source autopilot loaded with default quadcopter settings, in stabilize mode. Vibration data was collected based on a skilled human operator attempting to hover the drone at a constant position without the aid of height detecting hardware.

The vibrations generated by the motors exhibit different frequencies corresponding to different physical phenomena. For example, a motor spinning at 100 Hz will exhibit a 100 Hz fundamental signal and harmonics of that signal. Unfortunately, the motor will also cause a DC shift in acceleration data despite the motor not exhibiting 0 Hz acceleration. This effect is well understood and modeled due to second order non-linearity in MEMs accelerator behavior [23]. To account for this effect and properly interpret the AC acceleration data, the mean value of the entire sample size was subtracted from the entire sample to remove the DC data.

Using the setup above, 1000 samples of acceleration data can be collected per second (hereby called 1 data point). Each experiment will be run for 10 seconds to collect 10 data points. Every second, a Fourier Fast Transform algorithm is applied to the collected data with a window size of 1000. The data is then plotted in both time and frequency domains in MATLAB, using the fft() function. The 10 FFT results are then averaged. An inverse FFT is then applied on the aggregate FFT to get back the average time domain vibration spectrum.

In the table below, we summarize the entire set of vibration data obtained. Each cell in the table denotes the experiment conditions. 10 samples were obtained for each experiment. The cells that are struck out were deemed to be experimentally unfeasible to be carried out due to safety reasons when the vibration got too intense. The aggregated FFT and time domain plots are shown in the next section.

	No load	Loaded	Loaded, loose pylon	Loaded, loose motor	Loaded, broken propeller	
Pulse width (us)	800	800	800	800	800	Low speed
	900	900	900	900	900	
	1600	1600	1600	1600	~~1600~~	Medium speed
	1700	1700	1700	~~1700~~	~~1700~~	
	2200	2200	2200	~~2200~~	~~2200~~	High speed
	2300	2300	2300	~~2300~~	~~2300~~	

Table 1: Test cases.

III: RESULTS

Proper motors

In this sub-section, the plots of motors working properly are plotted. First, plots of the unloaded motor spinning at low speeds are labeled 800us_unloaded and 900us_unloaded respectively, where 800us and 900us denote the pulse width. The speeds are increased and the plots for 1600us, 1700us, 2200us and 2300us are shown on the next page.

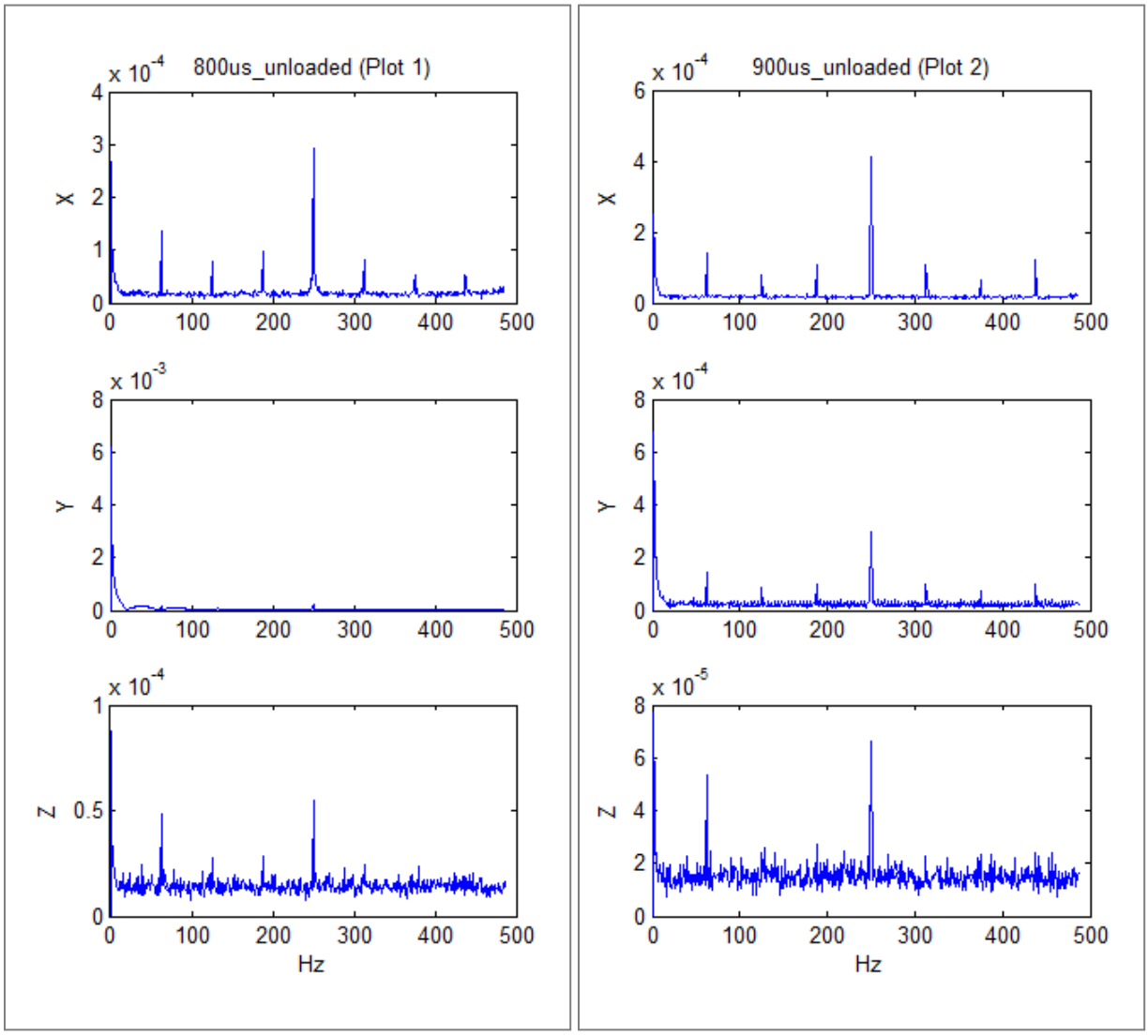

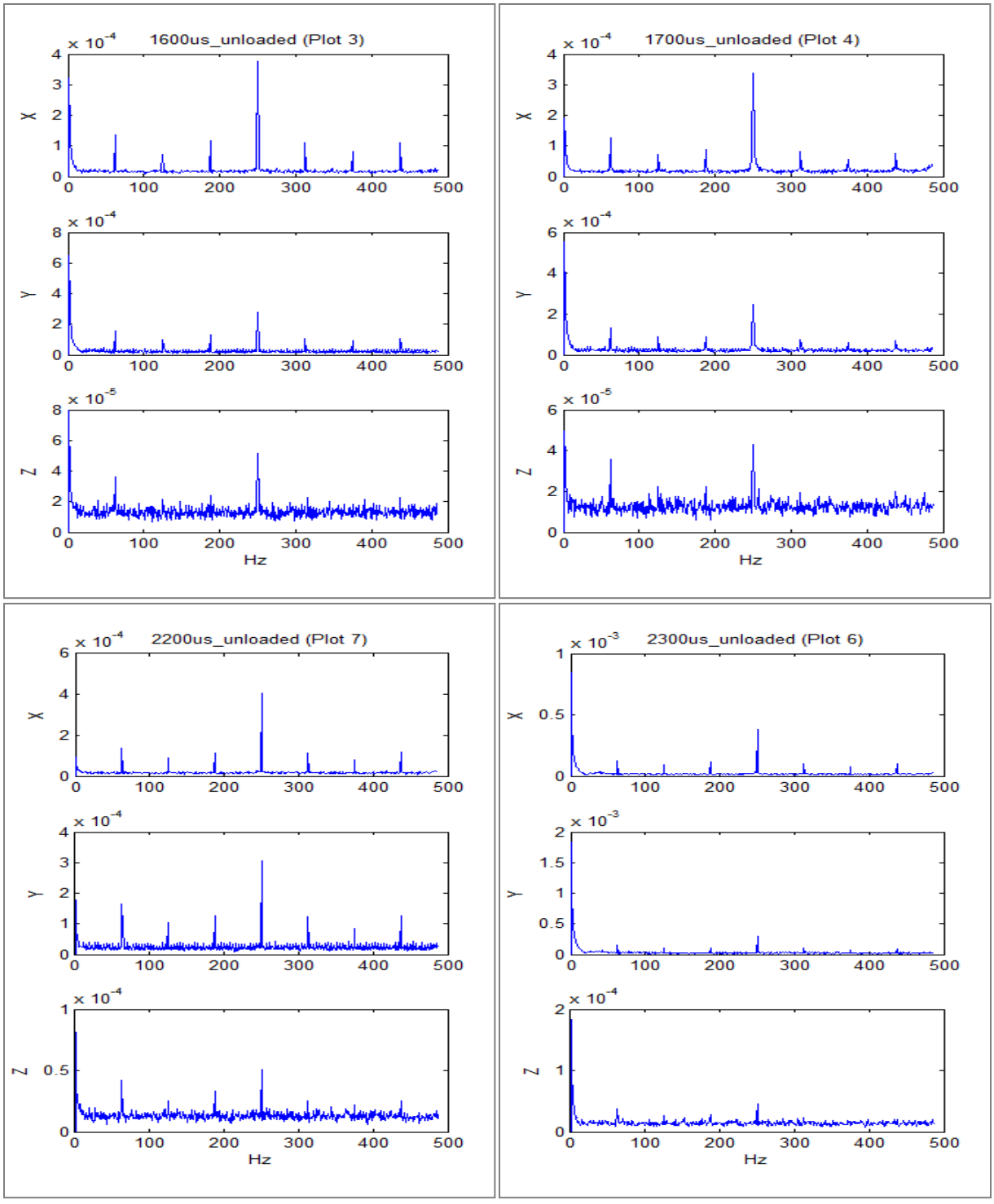
1600us_unloaded (Plot 3)
1700us_unloaded (Plot 4)
2200us_unloaded (Plot 7)
2300us_unloaded (Plot 6)
X
Y
Z
Hz

The next 6 panels show the motors with propellers attached on, with the same speed settings. Note the change in scale for the vertical axes for different plots.

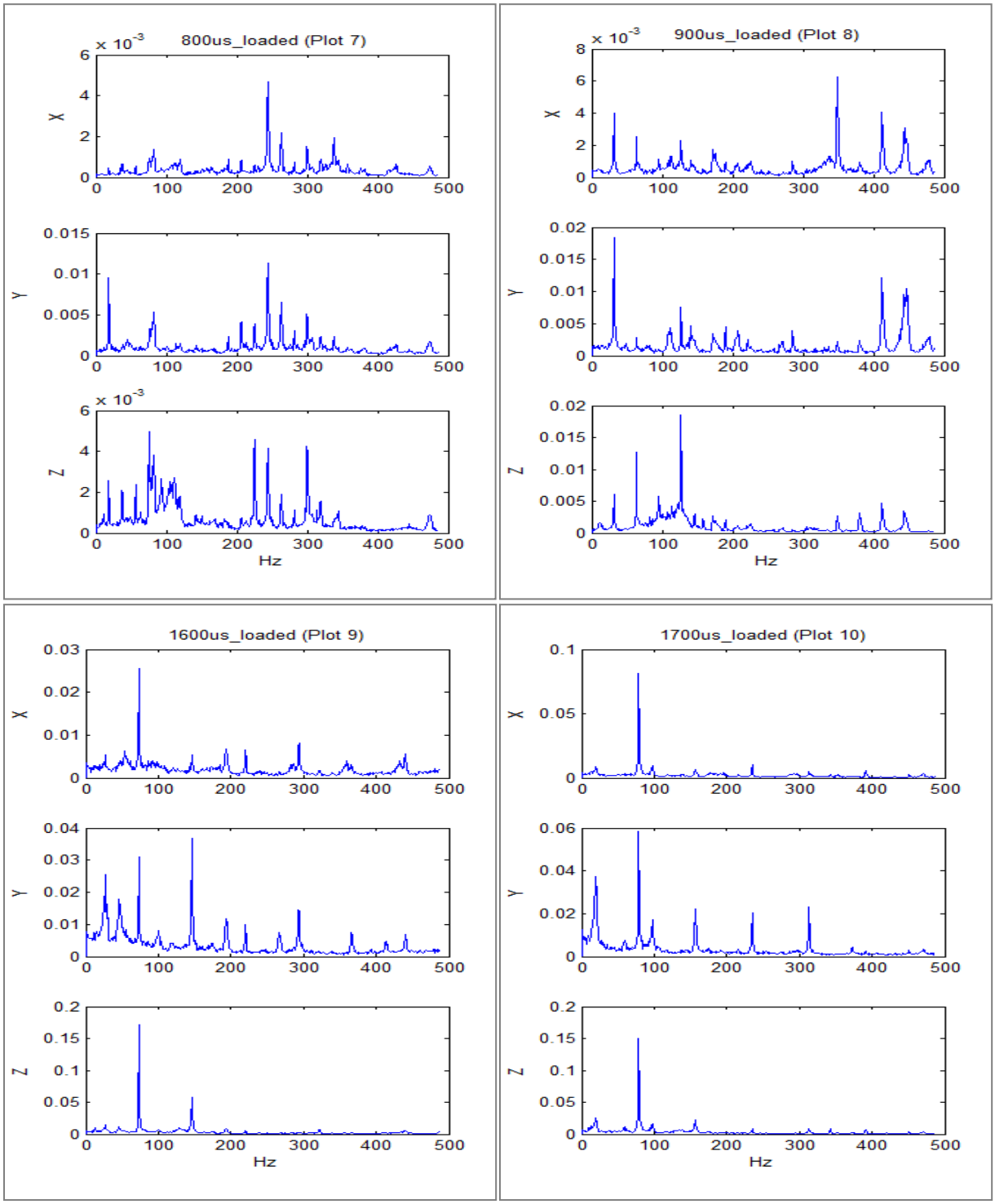

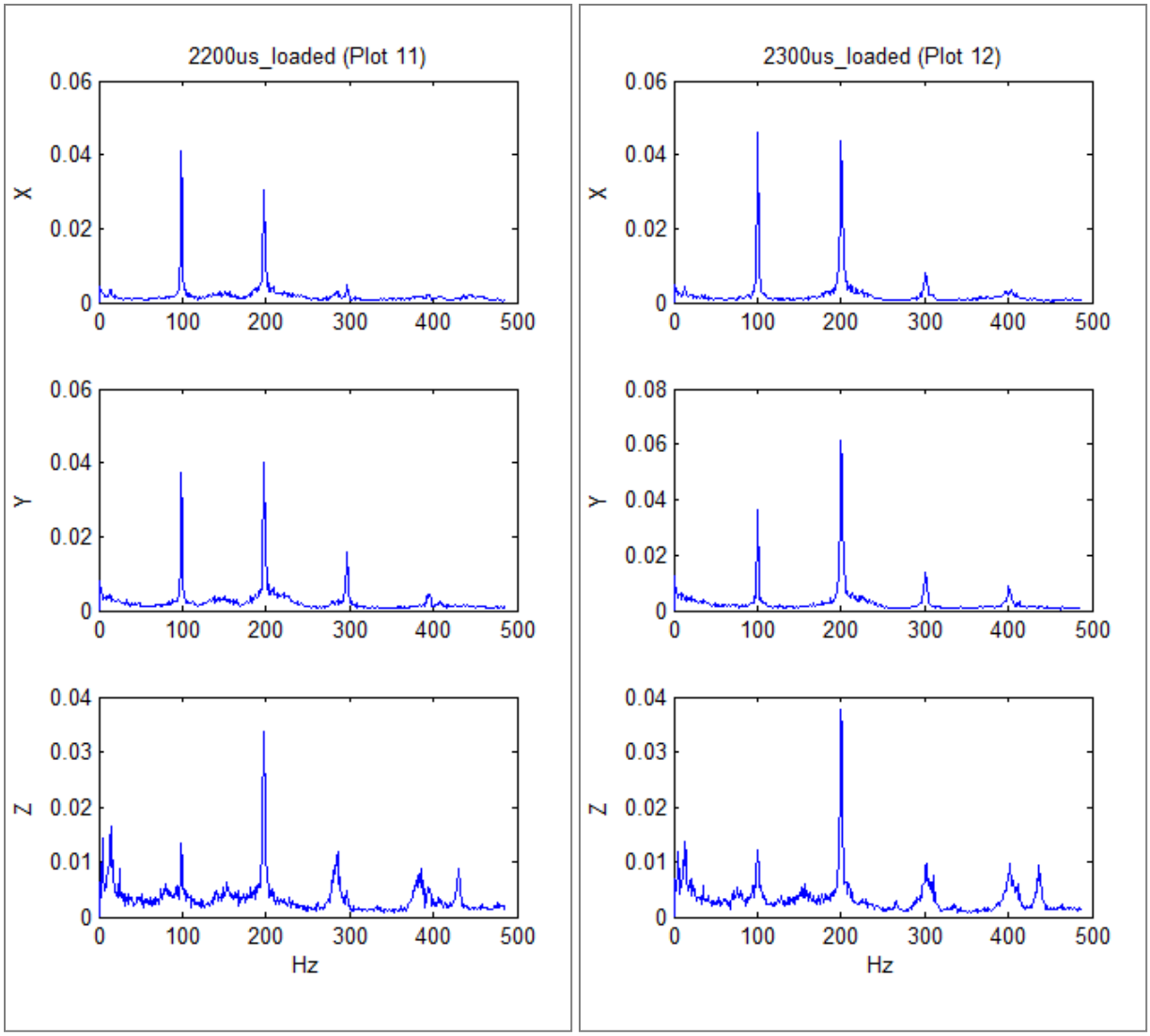

Defective situations

Next, we have situations where the pylon is loose. The FFT figures are titled accordingly to indicate the PWM pulse width.

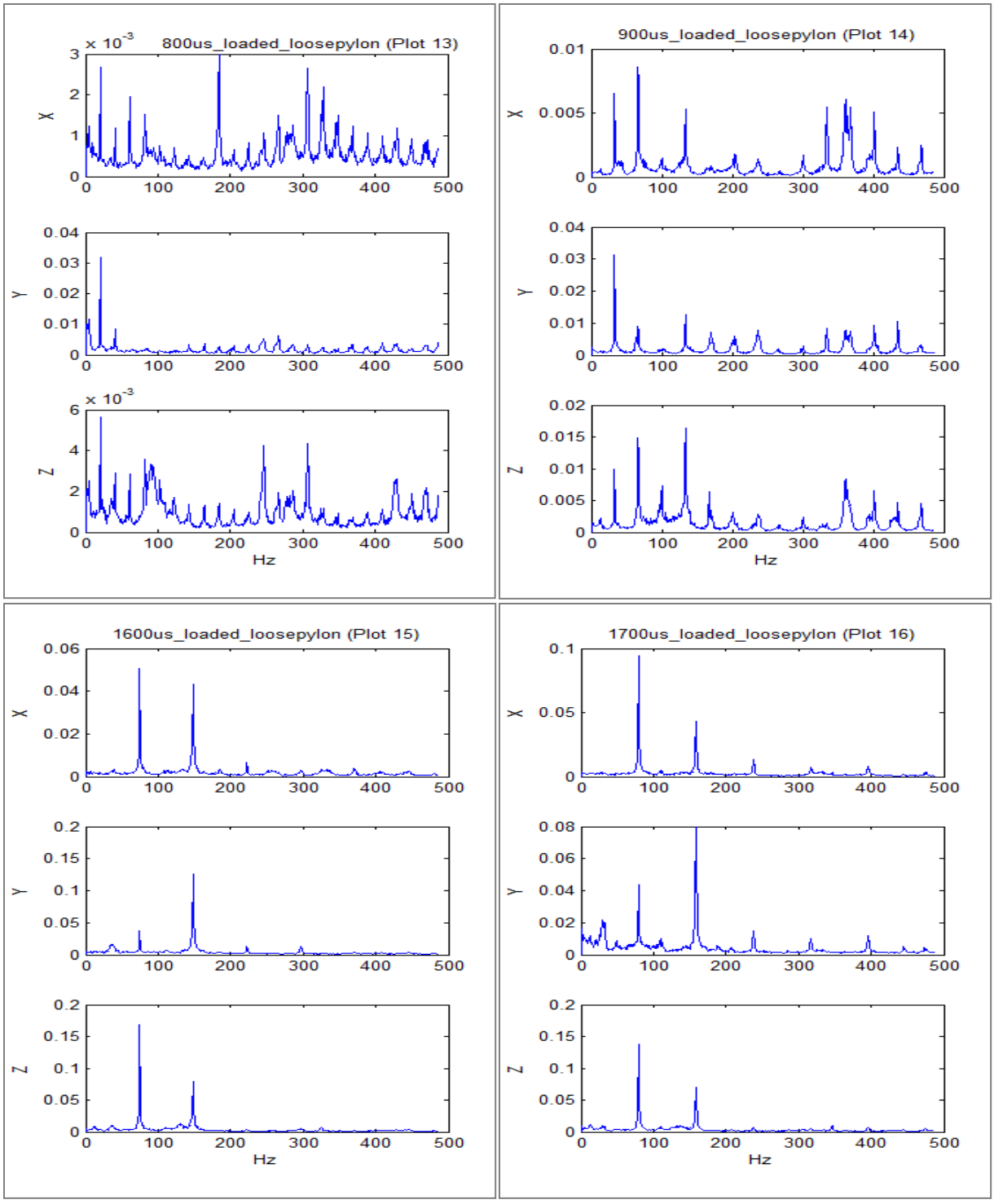
800us_loaded_loosepylon (Plot 13)
900us_loaded_loosepylon (Plot 14)
1600us_loaded_loosepylon (Plot 15)
1700us_loaded_loosepylon (Plot 16)
X
Y
Z
Hz
x 10^-3

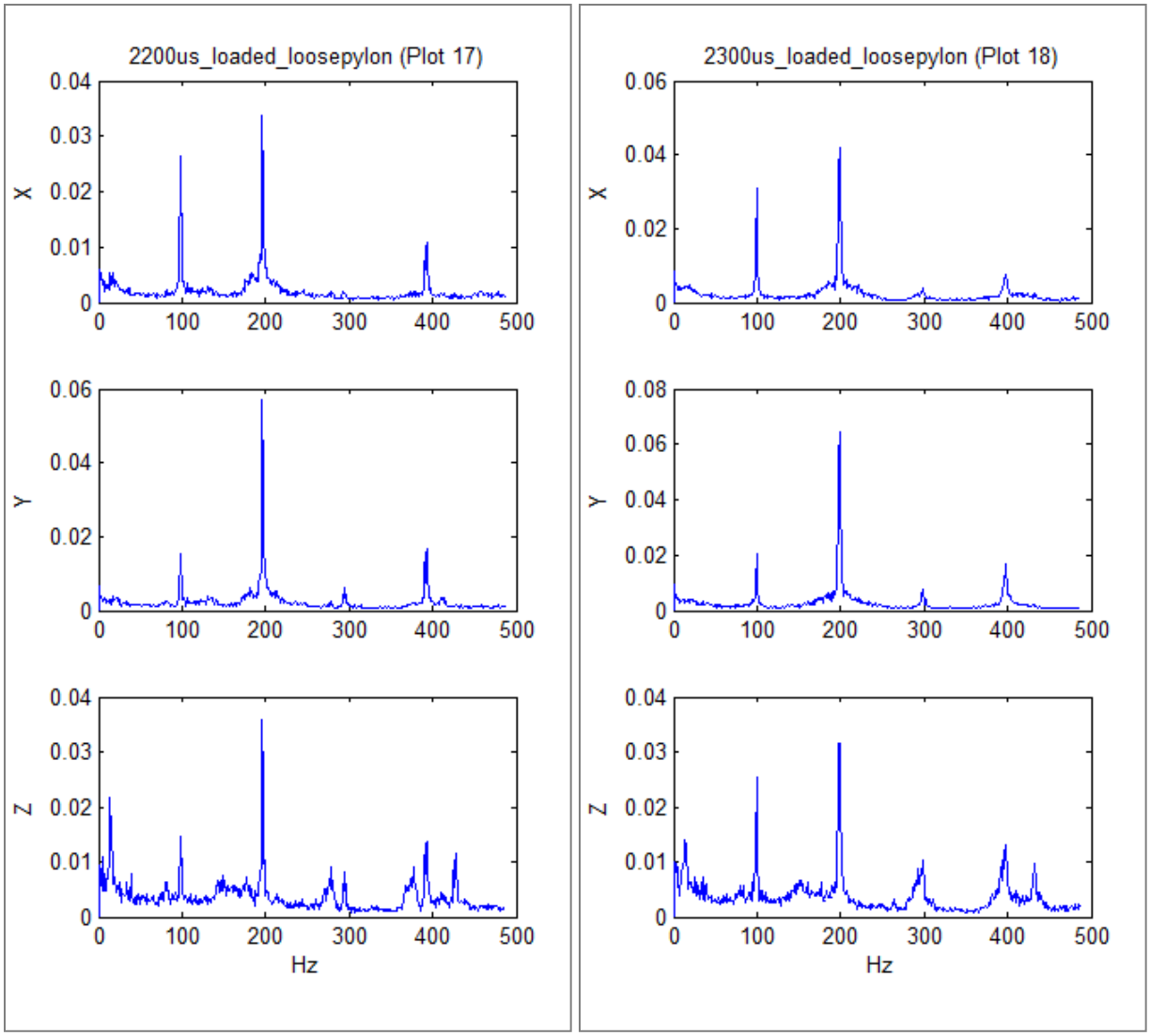

Next, we have plots where the screws holding down the motor assembly to the arms are loose. The speed is not increased further for safety reasons: the motor assembly was wobbling too much and starting to wear down the screws. After that, the plots of the spectrum for a motor spinning with a broken propeller are shown. Only two speeds were tested for safety reasons. As the speed was increased, the y-direction wobbling got too big, compromising the safety of the clamping structure. Thus, some tests were struck off the list in table 1. Finally, the plot of an actual flying quadcopter was shown as well.

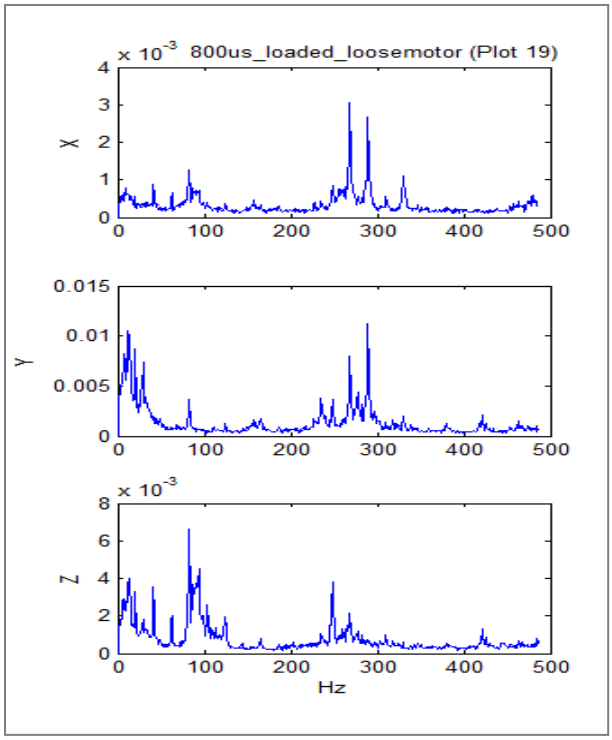
800us_loaded_loosemotor (Plot 19)
X
Y
Z
Hz

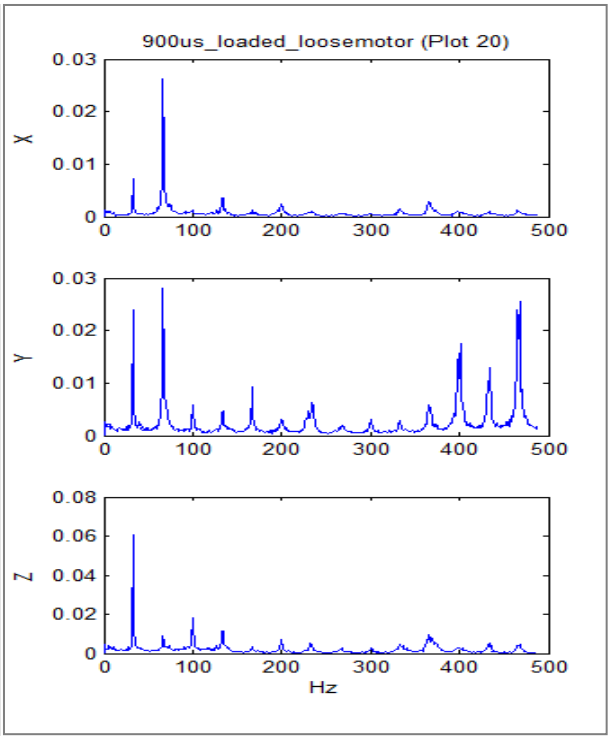
900us_loaded_loosemotor (Plot 20)
X
Y
Z
Hz

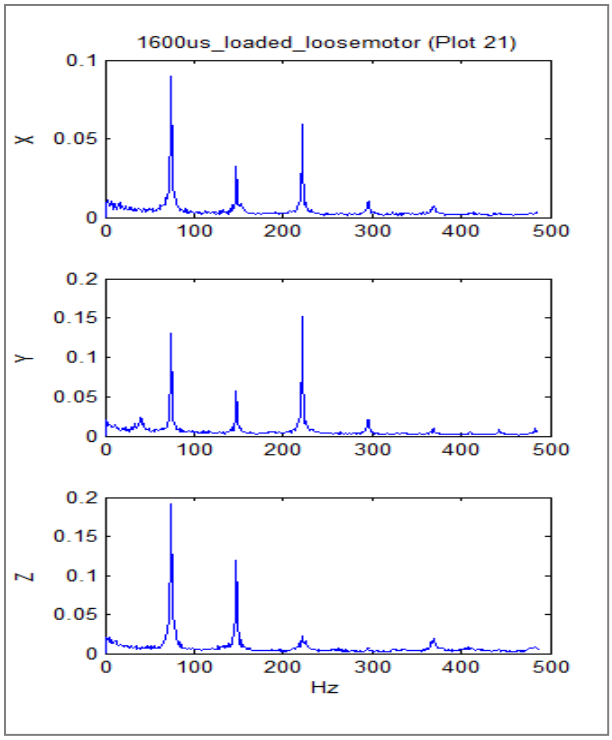
1600us_loaded_loosemotor (Plot 21)
X
Y
Z
Hz

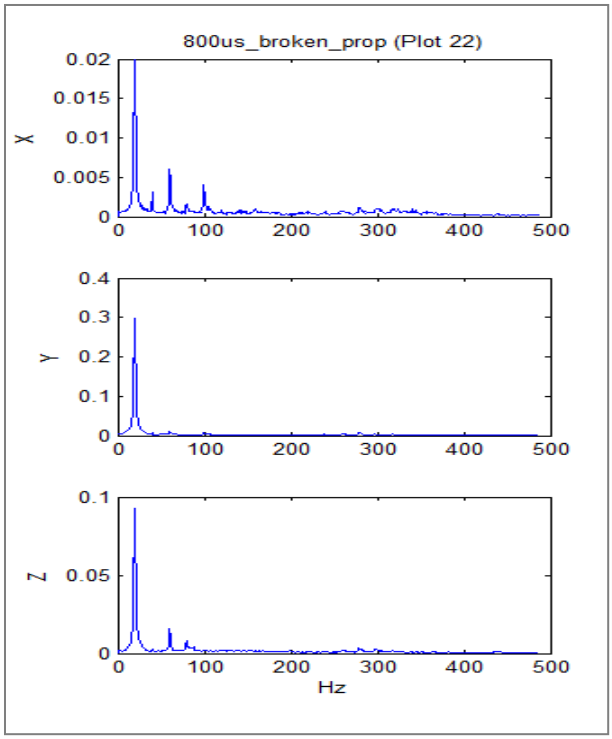
800us_broken_prop (Plot 22)
X
Y
Z
Hz

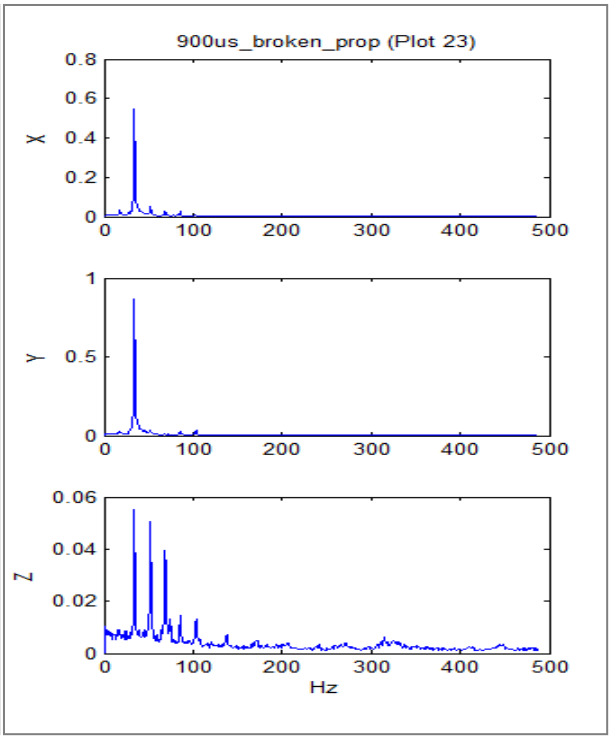
900us_broken_prop (Plot 23)
X
Y
Z
Hz

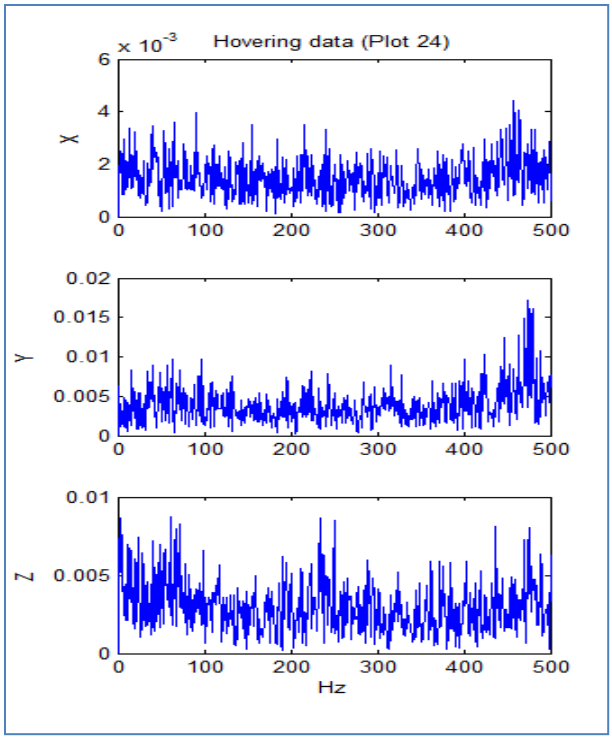
Hovering data (Plot 24)
X
Y
Z
Hz

IV: DISCUSSION AND IMPLICATIONS

In this section, we take a look at motors with loose pylons, loose motors, and finally broken propellers in that order. In general, the y-direction acceleration data is the most useful. This is because in the static tests, the clamping down of the airframe serves to attenuate and amplify different frequencies and mode shapes in the z and x directions. When the motors start generating maximum thrust, they started creating oscillations due to the z-direction stiffness of the cantilevers. These vibrations are not a reflection of motor or structural failure. However, the y-direction vibrations are less susceptible to be affected by the clamped condition, because given the setup, the motors do not generate enough y-direction acceleration to generate forces against the experimental set up (i.e. the clamp holding down the drone). Thus, in general for the results, we will analyze the y-direction acceleration unless otherwise stated.

Loose pylons

In the cases with the loose pylons, all of the defective situations demonstrated significantly higher 2^{nd} harmonic y-direction acceleration. First, we look at the low speed cases, plot 7 vs. 13 and 8 vs. 14. The fundamental frequencies are about 19 Hz and 31 Hz respectively, giving us a 2^{nd} harmonic of about 38 Hz and 62 Hz. Observing the 2^{nd} harmonic frequencies in plots 13 and 14 show a significantly increased 2^{nd} harmonic vibration.

The above observation is not just confined to the cases at low speeds. Looking at the medium throttle cases (plots 9 vs. 15 and plot 10 vs. 16), we see fundamental frequencies of 73 Hz and 78 Hz respectively, giving us 2^{nd} harmonics of 146 Hz and 156 Hz. Looking at plots 15 and 16, we do see that the 2^{nd} order harmonic has increased substantially, by a factor of 3-4. Similarly, in the high speed cases (plots 11 vs. 17 and plots 12 vs. 18), we get fundamental frequencies of 198 Hz and 200 Hz respectively, yielding 2^{nd} harmonics of 396 Hz and 400 Hz. In

the 2200 us case, the fundamental vibration doubled in magnitude, but the 2nd harmonic *quadrupled*. In the 2300 us case, the fundamental stayed roughly the same, but the 2nd harmonic doubled.

It appears that the presence of defects on the motor generates more non-linearity. In general, as well will see in other cases, the defects cause more vibration. In this case, the increased vibrations show up as higher magnitudes in the harmonics. In most of the cases listed below, however, these vibrations show up as large amplitude oscillations at low frequencies.

Loose motors

When the motors were loosely connected to the airframe, two key differences were observed. At a PWM period of 800 us when the motor is spinning at its lowest speed setting, the introduction of a loose motor resulted in a rich amount of low frequency components in the y-direction. A comparison of plots 7 and 19 reveal that at low frequencies, the loose motor introduced vibrations with a wideband characteristic from 0 to approximately 70 Hz. This low frequency vibration was visually seen. It is also mixed to higher frequencies, resulting in an envelope around the 230-300 Hz region. The region is circled in the next diagram.

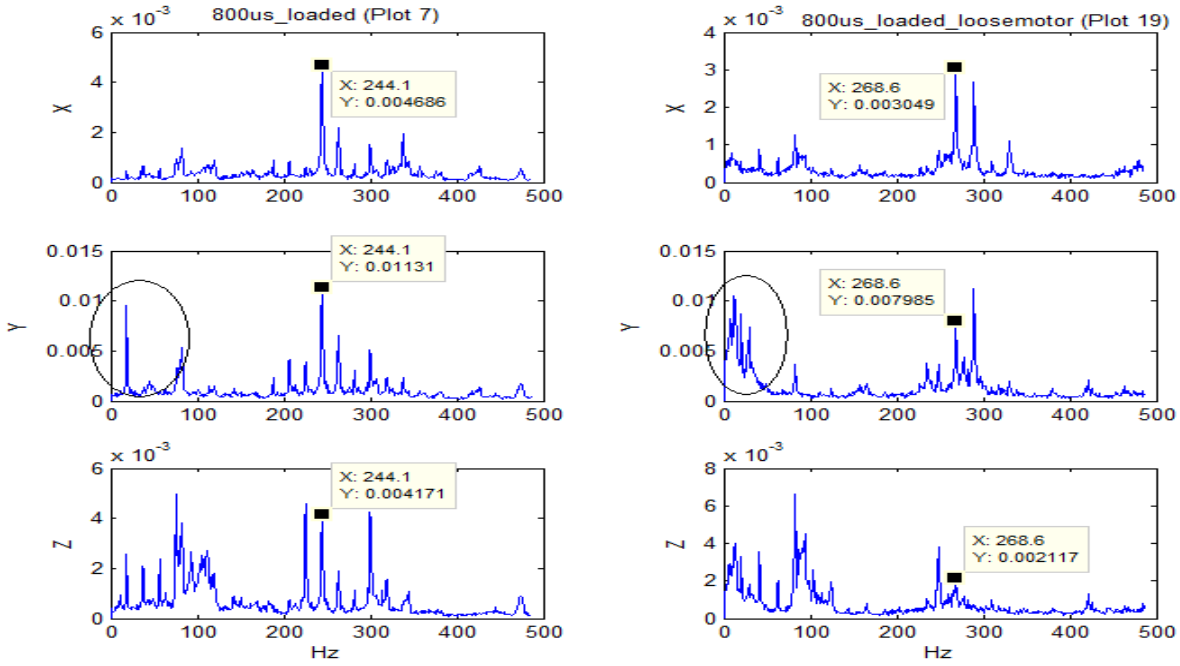

As the throttle was increased, the difference changed from being a wideband vibration signature to a narrowband, high intensity vibration. At 900us/20000us and 1600us/20000us PWM pulses respectively, there is a marked increase in spectrum power. Comparing plot 8 and 20, we see that at is a large peak at 33 Hz in the z-direction vibration. In the x-direction, a new vibration at 66 Hz also shows up with a huge increase in magnitude over the normal motors. When the speed was increased to 1600us, the y-direction magnitudes increased by factors of 3-4 and showed new frequency content.

Broken Propellers

When the propellers were broken, there were very large oscillations generated due to the unbalanced torque on the propellers. The motors were only spun at 2 low speeds, given only 800us and 900us PWM signals. The peak oscillations showed up as low frequency (20 – 30 Hz) vibrations with large magnitudes. For example, at a PWM pulse of 800 us (compare plots 7 and 22), the 19 Hz vibration was 0.3g on the y-axis, 30 times that of normal operation. In the 900 us

case (compare plots 8 and 23), the 34 Hz oscillation was a whooping 40 times that of normal operation. It appears that the airframe was resonating and started to fail, so no more data points were obtained.

This experiment demonstrated the ability of this vibration sensing technique to detect unbalanced propellers. When a propeller is unbalanced, the torque generated during each cycle of the motor generates a periodic y-direction force on the airframe as a consequence of Newton's 3rd Law of Motion. In this case, the propeller was grossly unbalanced due to the broken edge, hence resulting in a large amplitude oscillation that can be visually observed without the acceleration data. However, in less extreme cases, this technique would be able to identify when the propeller is moderately unbalanced. This is advantageous for users of UAS to take preemptive steps to prevent premature failure of their airframe. By swapping out unbalanced propellers, users will be able to reduce the vibration contact forces on the screws, joints and bearings on an airframe, improving the lifespan of a UAS.

In each of the different defect mechanisms discussed above, it is fairly straightforward to detect problems in the motors or airframe. Hence, it is a relatively easy task to implement a controller to check for potential errors preflight. For example, the flight computers might be made to check the spectrum near each motor before the start of each flight. If the vibrations are too large or the 2nd harmonics get above a certain threshold, the flight computer may disarm the UAS and prevent flight.

Despite the relative ease of spotting problems through the vibration spectrum, it is harder to analyze actual flight data for two reasons. First, as 4 propellers are used in a quadcopter, there is a transmission of vibration from one motor to the other three motors. This results in both additive and multiplicative relations between the different vibration modes, greatly complicating

the spectrum. A look at plot 24, depicting actual flight data, shows that while the overall shape and magnitudes follows the motors in plot 8 relatively closely, the spectrum is much richer. Thus, in order to diagnose any problem using frequency harmonics, it becomes virtually impossible to determine which motor is generating which harmonic without knowing the exact motor speeds. Fortunately, we can still tell if the magnitudes are getting too big, as in the case of loose parts.

We note that the results above are for a specific model of the motor, propeller, and airframe construction. With different motors, ESCs and propeller configurations, the vibration spectrum should look different. Nevertheless, with this demonstration, it is possible to implement a low cost warning system on board UAS. In the experiment carried out above, there was no dedicated IMU to measure and transmit the data to the flight computer. However, in a hypothesized system, it is possible to make a low cost IMU board which implements the FFT calculations and then send the results to the flight computer by two long wires using I^2C. The flight computer would then decide whether or not the vibration threshold has been exceeded. Here is the architecture of the proposed system, which will be a stripped down version of the IMU used for this paper.

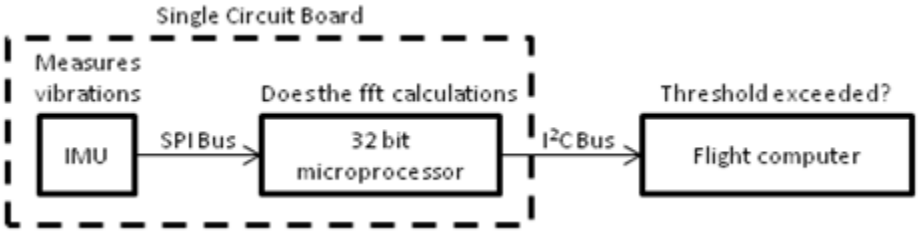

Figure 5. Hypothesized vibration monitoring on UAS.

Here is a breakdown of the cost of the parts used and the power consumption of the parts. The calculations are for a quadcopter, whereby each motor would require a CPU and an IMU to measure vibration data, so we would need 4 set ups.

Name of part required	Function	Cost per unit[1][2]	Qty per UAS	Subtotal Cost
LIS344ALHTR	MEMs accelerometer	$2.16 – $2.317 [24]	4	$8.64 – $9.268
MSP430F2618	Microprocessor	$7.143 – $12.97 [24]	4	$28.57 – $51.88
	Circuit Board	$1 – $3	4	$4 – $12
			Total	**$41.21 – $73.15**

Table 2: Cost of parts required

Function	Power per unit[3]	Qty per UAS	Subtotal power
MEMs accelerometer	2.24 mW [25]	4	8.86 mW
Microprocessor	24 mW [26]	4	96 mW
Circuit Board	-	4	-
		Total	**104.86 mW**

Table 3: Power consumption of sensors

The cost of providing such a sensing mechanism seems to be pretty high, as we see from table 2. However, we recall that the cost of a UAS crash due to malfunctioning structures can potentially be much higher due to the high cost of parts as well as liability costs. Furthermore, the cost of the circuit board has been estimated on the high side. If mass produced, the PCBs can cost even less, under $1 if manufactured offshore.

Furthermore, the power consumption of such a system is relatively low. Even though hundreds of mill watts is large for modern electronics, the figure given is a worst case estimate during measurement and when the microprocessor is running the FFT algorithm. Furthermore, 100mW is insignificant compared to the power consumption on the UAS motors, which can go

[1] For the the MEMs accelerometer and microprocessor, the price changes based on quantity purchased. The prices listed are the maximum and minimum to be expected

[2] For the printed circuit boards, the price greatly depends on the design of the final PCB, how it is to be shaped and how the components are to be mounted. The price range listed here is a high end estimate.

[3] The power consumption is provided as a worst case figure. The actual figure during usage is lower, depending on how the microcontroller and accelerometer are programmed during the intervals between measurements of data.

up to 200 W, a difference of 2000 times. The weight of each set up will also be insignificant, with each sensor and microprocessor only weighing several grams.

As such, with our series of empirical tests and comparisons, we believe that a relatively low cost and effective method for monitoring vibration can be implemented on UAS to mitigate the risks of structural failure. While we first need vibration data to generate the baseline conditions, once we are able to collect that data , it is fairly straightforward to interrupt the flight controller if the vibration magnitudes get too large, and have the UAS notify the ground control station to take evasive or precautionary steps.

V: CONCLUSION

An empirical method of observing the vibration spectrum of a UAS airframe was demonstrated by adopting motor vibration measurement methods. A baseline condition for what constitutes proper operation was first made at different motor speeds for a specific motor, and then compared against that of an operating motor on a UAS. Data from a UAS with 4 motors was shown, indicating similarities with the static test results.

Using the baseline results, one can infer when vibrations on the airframe on a UAS get too big and may compromise the structural integrity. As such, a user controlling a UAS will be able to get real time data when problems arise with the mechanical structure on the UAS. The relatively low cost and simplicity of such a measurement system makes it promising to be applied to small scale UAS.

Future work should analyze where the threshold to trigger a warning should be. In particular, instead of trying to decipher the spectrum of a motor failure, one may be able to use neural networks to analyze thousands of UAS flight data and learn to recognize when signs of failure are showing. Finally, future work should be done to compare the signals sent to the motor

against the actual rotation speed. If a motor is poorly oiled or has defects in its bearings or propellers, it may show up as a divergence between signals sent to it and the actual speed.

VI: ACKNOWLEDGEMENTS

The author would like to thank Professor Raja Sengupta from UC Berkeley for stimulating discussion and guidance throughout the course of this Master's Project. Also, special thanks go to 3D Robotics for loaning the equipment required for flying and testing the drones. The author would also like to thank Professor Kris Pister's group at UC Berkeley for agreeing to loan out their IMUs and Atmel RZUSBSticks. Finally, heartfelt thanks go to Fabien Chriam, a graduate student with Pister's group, for his guidance and advice on speeding up and optimizing the data collection process with the IMUs, Python and MATLAB scripts.

VII: LITERATURE CITED

[1] "Unmanned Aircraft Systems Roadmap 2005-2030." *Federation of American Scientists*. Office of the Secretary of Defense, n.d. Web. 3 Apr. 2014. <http://www.fas.org/irp/program/collect/uav_roadmap2005.pdf>.

[2] "Up in the air." *The Economist*. The Economist Newspaper, 29 Mar. 2014. Web. 3 Apr. 2014. <http://www.economist.com/news/special-report/21599524-drones-will-change-warand-more-up-air>.

[3] Hart, Benjamin. "Drones Could Revolutionize Agriculture, Farmers Say." *The Huffington Post*. TheHuffingtonPost.com, 14 Dec. 2013. Web. 3 Apr. 2014. <http://www.huffingtonpost.com/2013/12/14/drones-agriculture_n_4446498.html>.

[4] Sharma, Rakesh. "Growing The Use Of Drones In Agriculture." *Forbes*. Forbes Magazine, 26 Nov. 2013. Web. 3 Apr. 2014.

<http://www.forbes.com/sites/rakeshsharma/2013/11/26/growing-the-use-of-drones-in-agriculture/>.

[5] Sheets, Connon Adarms. "China Beat Amazon Prime Air To The Commercial Drone Delivery Market."*International Business Times*. N.p., 2 Dec. 2013. Web. 3 Apr. 2014. <http://www.ibtimes.com/china-beat-amazon-prime-air-commercial-drone-delivery-market-1491636>.

[6] Kelly, Heather. "Beer-delivery drone grounded by FAA." *CNN*. Cable News Network, 3 Feb. 2014. Web. 3 Apr. 2014. <http://edition.cnn.com/2014/01/31/tech/innovation/beer-drone-faa/>.

[7] "The Economic Impact of Unmanned Aircraft Systems Integration." auvsi.org. Web. 2 Feb. 2014. <http://higherlogicdownload.s3.amazonaws.com/AUVSI/958c920a-7f9b-4ad2-9807-f9a4e95d1ef1/UploadedImages/New_Economic%20Report%202013%20Full.pdf>.

[8] "Economic Report." - Association for Unmanned Vehicle Systems International. Web. 2 Feb. 2014. <http://www.auvsi.org/resources/economicreport>.

[9] Cooper, Aaron, Carol Cratty, and Rob Frehse. "Drone came within 200 feet of airliner over New York." *CNN*. Cable News Network, 5 Mar. 2013. Web. 3 Apr. 2014. <http://edition.cnn.com/2013/03/04/us/new-york-drone-report/index.html>.

[10] "Integration of Civil Unmanned Aircraft Systems (UAS) in the National Airspace System (NAS) Roadmap." *Federal Aviation Authority*. N.p., 7 Nov. 2013. Web. 3 Apr. 2014. <http://www.faa.gov/about/initiatives/uas/media/UAS_Roadmap_2013.pdf>.

[11] "Model Aircraft Operating Standards." *Advisory Circular*. Department of Transportation, Federal Aviation Administration, n.d. Web. 3 Apr. 2014. <http://rgl.faa.gov/Regulatory_and_Guidance_Library/rgAdvisoryCircular.nsf/0/1acfc3f689769a56862569e70077c9cc/$FILE/ATTBJMAC/ac91-57.pdf>.

[12] "Ceres Imaging." *Ceres Imaging*. N.p., n.d. Web. 3 Apr. 2014. <http://www.ceresimaging.net/>.

[13] "Strength, Safety and Reliability." *Skycatch*. N.p., n.d. Web. 3 Apr. 2014. <https://www.skycatch.com/product>.

[14] "APMs Failsafe Function." *ArduPlane*. N.p., n.d. Web. 3 Apr. 2014. <http://plane.ardupilot.com/wiki/arduplane-setup/apms-failsafe-function/>.

[15] Meyer, L. D., F. F. Ahlgren, and B. Weichbrodt. "An Analytic Model for Ball Bearing Vibrations to Predict Vibration Response to Distributed Defects." *Journal of Mechanical Design* 102.2 (1980): 205. Print.

[16] Sunnersjö, C.s.. "Rolling bearing vibrations—The effects of geometrical imperfections and wear." *Journal of Sound and Vibration* 98.4 (1985): 455-474. Print.

[17] Randall, R.b.. "Detection and diagnosis of incipient bearing failure in helicopter gearboxes."*Engineering Failure Analysis* 11.2 (2004): 177-190. Print.

[18] Ma, J., and C.j. Li. "Gear Defect Detection Through Model-Based Wideband Demodulation Of Vibrations." *Mechanical Systems and Signal Processing* 10.5 (1996): 653-665. Print.

[19] Schoen, R.r., T.g. Habetler, F. Kamran, and R.g. Bartfield. "Motor bearing damage detection using stator current monitoring." *IEEE Transactions on Industry Applications* 31.6 (1995): 1274-1279. Print.

[20] Riley, C.m., B.k. Lin, T.g. Habetler, and R.r. Schoen. "A method for sensorless on-line vibration monitoring of induction machines." *IEEE Transactions on Industry Applications* 34.6 (1998): 1240-1245. Print.

[21] Tandon, N, and A Choudhury. "A review of vibration and acoustic measurement methods for the detection of defects in rolling element bearings." *Tribology International* 32.8 (1999): 469-480. Print.

[22] "GINA - OpenWSN - Confluence." *GINA - OpenWSN - Confluence*. N.p., n.d. Web. 9 Apr. 2014. <https://openwsn.atlassian.net/wiki/display/OW/GINA>.

[23] Senturia, Stephen D.. *Microsystem design*. Boston: Kluwer Academic Publishers, 2001. 503-505. Print.

[24] "Electronic Components." *Electronic Parts, Components and Suppliers*. N.p., n.d. Web. 10 Apr. 2014. <http://www.digikey.com/product-search/ >.

[25] "LIS344ALH: MEMS inertial sensor high performance 3-axis ±2/±6g ultracompact linear accelerometer." *ST Mircoelectronics*. N.p., n.d. Web. 10 Apr. 2014. <http://www.st.com/web/en/resource/technical/document/datasheet/CD00182781.pdf>.

[26] "Mixed Signal Microcontroller: MSP430F261X." *Texas Instruments*. N.p., n.d. Web. 10 Apr. 2014. <http://www.ti.com/lit/ds/symlink/msp430f2618.pdf>.